Histone Deacetylase-Dependent Establishment and Maintenance of Broad Low-Level Histone Acetylation within a Tissue-Specific Chromatin Domain†

Hogune Im,‡ Jeffrey A. Grass,‡ Heather M. Christensen,§ Andrew Perkins,|| and Emery H. Bresnick*,‡

Department of Pharmacology, Molecular and Cellular Pharmacology Program, University of Wisconsin Medical School, 383 Medical Science Center, 1300 University Avenue, Madison, Wisconsin 53706, Department of Cell Biology and Physiology, Washington University School of Medicine, 660 South Euclid Street, St. Louis, Missouri 63110, and Department of Physiology, Monash University, Wellington Road, Clayton, 3800 Victoria, Australia

Received September 3, 2002; Revised Manuscript Received October 2, 2002

ABSTRACT: The murine β-globin locus in adult erythroid cells is characterized by a broad pattern of erythroid-specific histone acetylation. The embryonic β-globin genes *Ey* and *βH1* are located in a ~30 kb central subdomain characterized by low-level histone acetylation, while the fetal/adult genes *βmajor* and *βminor* and the upstream locus control region reside in hyperacetylated chromatin. Histone deacetylase (HDAC) inhibitors induce H4 acetylation at the *Ey* promoter [Forsberg, E. C., Downs, K. M., Christensen, H. M., Im, H., Nuzzi, P. A., and Bresnick, E. H. (2000) *Proc. Natl. Acad. Sci. U.S.A. 97*, 14494−14499], indicating that HDACs maintain low-level H4 acetylation at this site. Since little is known about the establishment of broad histone modification patterns, we asked whether this mechanism applies only to the promoter or to the entire subdomain. We show that the HDAC inhibitor trichostatin A induces H4 hyperacetylation at multiple sites within the subdomain in erythroid cells. The hematopoietic factors p45/NF-E2, GATA-1, and erythroid kruppel-like factor (EKLF), which function through *cis* elements of the β-globin locus, were not required for induction of H4 hyperacetylation. Analysis of chromatin structure within the subdomain revealed low accessibility to restriction endonucleases and nearly complete CpG dinucleotide methylation. Induction of H4 hyperacetylation did not restore hallmark features of transcriptionally active chromatin. We propose that an HDAC-dependent surveillance mechanism counteracts constitutive histone acetyltransferase (HAT) access, thereby maintaining low-level H4 acetylation throughout the subdomain.

Organization of DNA into chromatin has important implications for establishing cell- and tissue-specific patterns of gene expression (*1*). The simplest level of chromatin structure, the nucleosome, consists of DNA wrapped 1.7 times around a core histone octamer (*2*, *3*). While nucleosomal DNA is accessible to certain DNA binding proteins, others are unable to overcome steric restrictions imposed by the nucleosome (*4*−*6*). Nucleosome arrays fold into higher-order structures that are stabilized by the linker histone H1 (*2*, *7*, *8*). Higher-order folding is a dynamic process (*9*) that severely restricts access of DNA binding proteins to the DNA. Chromatin structure is commonly analyzed by use of chromatin solubilized from nuclei via nucleolytic digestion and chromatin reconstituted on recombinant templates (*10*). While these approaches have yielded a wealth of structural and functional information, additional strategies are required to study chromosomal segments termed domains, in which many mammalian genes reside.

Although the concept of a chromatin domain was developed years ago (*11*), many questions remain regarding principles governing domain structure and transcriptional control within domains. "Active" chromatin is characterized by enhanced susceptibility to cleavage by DNase I, referred to as general DNase I sensitivity (*12*, *13*). Chromatin that exhibits general DNase I sensitivity is ~2-fold more sensitive to cleavage than "inactive" chromatin. Although the molecular basis for the sensitivity is unknown, it can coincide with the distribution of acetylated histone H4 (*14*). Histone acetylation increases accessibility of nucleosomal DNA (*15*, *16*), presumably due to structural transitions within the nucleosome. However, hyperacetylation does not induce nucleosome disassembly (*17*−*20*). Histone acetylation also inhibits higher-order chromatin folding (*21*). As only a 3-fold increase in acetylation prevents higher-order folding in vitro (*22*), small changes in acetylation elicit major consequences. Given the extensive evidence linking histone acetylation with the control of transcription and other nuclear processes (*23*−*28*), it is critical to understand how acetylation functions at the level of chromatin domains in vivo.

The β-globin locus is used as a model for studying transcriptional control within domains (*29*, *30*). Acetylated histones H3 and H4 are distributed broadly throughout the chicken β-globin locus in erythroid cells, in which the β-globin genes are active (*14*, *31*). Even though the cluster contains genes active exclusively during embryogenesis or in the adult, the entire cluster is hyperacetylated. It was

† This work was supported by NIH DK50107. E.H.B. is a Leukemia Society of America Scholar, a Shaw Scientist, and a Romnes Scholar.

* To whom correspondence should be addressed: Telephone 608-265-6446; fax 608-262-1257; e-mail ehbresni@facstaff.wisc.edu.

‡ University of Wisconsin Medical School.

§ Washington University School of Medicine.

|| Monash University.

10.1021/bi026786q CCC: $22.00
Published on Web 11/26/2002

hypothesized that acetylation renders the domain transcriptionally competent (*14*). By contrast, the murine β-globin locus has a nonuniform acetylation pattern in adult erythroid cells (*32*, *33*). Acetylated H3 and H4 are enriched at the LCR,[1] which mediates high-level transcription of the β-globin genes (*34*, *35*), and at the fetal/adult β-globin genes (*βmajor* and *βminor*). The embryonic β-globin genes (*Ey* and *βH1*) reside within a ~30 kb central subdomain characterized by nearly undetectable levels of H3 acetylation and low-level H4 acetylation. We hypothesized that formation of this subdomain is essential for silencing the embryonic β-globin genes during erythropoiesis (*32*). Consistent with this prediction is the fact that the *βH1* promoter is hyperacetylated in 10.5-day postconception yolk sac (*32*), which is enriched in embryonic erythroid cells. Thus, factors that establish the subdomain would be critical silencing determinants. Additional evidence exists in support of a unique chromatin structure at the *Ey* and *βH1* genes (*36*). Chromatin at *Ey* and *βH1* is insensitive to DNase I, while chromatin at *βmajor* and *βminor* is DNase I-sensitive. Subdomains differing in DNase I sensitivity have also been detected within the human β-globin locus (*37*).

What mechanisms establish and maintain low-level acetylation across a broad chromosomal region? HAT access might be restricted, or HDACs might efficiently remove the acetylation. Activators and repressors recruit HATs (*38*) and HDACs (*39*, *40*), respectively, via protein−protein interactions, resulting in local chromatin modification. Certain activators, such as the thyroid hormone receptor (*41*), can also recruit HDACs. It is unclear, however, whether establishment of broad acetylated and hypoacetylated regions requires targeted recruitment or a different mechanism. Of relevance to this issue is the finding that the Spt−Ada−Gcn5 activator (SAGA) complex, containing the GCN5 HAT, induces local H3 acetylation, while the NuA4 HAT induces broader H4 acetylation *in vitro* (*42*). Establishment of broad acetylation might therefore require specialized HATs and HDACs, with differing abilities to act over a distance on a chromosome.

Regarding the *Ey* promoter that resides within the central subdomain, we asked whether inhibiting HDACs with butyrate restores acetylation (*32*). Butyrate inhibits multiple HDACs but not Sir2p (*43*), HDAC6 (*44*), and HDAC10 (*45*). Butyrate preferentially induced H4 acetylation at the *Ey* promoter, suggesting that HDACs establish and maintain low-level H4 acetylation. Establishment and maintenance of H3 hypoacetylation involves a distinct mechanism, either impaired access of HATs that establish H3 acetylation or involvement of inhibitor-resistant HDACs that maintain H3 hypoacetylation.

We tested herein whether HDACs maintain low-level H4 acetylation throughout the central subdomain and whether induction of H4 hyperacetylation stimulates other chromatin structure changes. The results are discussed in the context of a model of how the central subdomain assembles.

EXPERIMENTAL PROCEDURES

Cell Culture. MEL (*46*), p45/NF-E2-null CB3 (*47*), and L1210 lymphocytic leukemia (*48*) cells were maintained in Dulbecco's modified Eagle's medium (DMEM) (Biofluids) containing 1% antibiotic/antimycotic (Gibco/BRL) and 5% calf serum, 5% fetal calf serum (MEL/L1210), or 10% fetal calf serum (CB3). EKLF-null B1 cells (*49*) were maintained in DMEM containing 10% fetal calf serum and 1% glutamine. GATA-1-null G1E cells (*50*) were maintained in Iscove's modified Dulbecco's medium (IMDM) (Gibco/BRL) containing 15% fetal calf serum, 2% penicillin−streptomycin (Gibco/BRL), 2 units/mL erythropoietin, 120 nM monothioglycerol (Sigma), and 0.6% conditioned medium from a kit ligand-producing Chinese hamster ovary (CHO) cell line. Cells were grown in a humidified incubator at 37 °C in the presence of 5% carbon dioxide. In certain experiments, cells were incubated with 165 nM TSA or vehicle for 4 h. This treatment induced bulk H3 and H4 hyperacetylation, as detected by Western blot analysis of acid-extracted histones with antibodies that react with multiple acetylated forms of H3 and H4 (data not shown). To inhibit DNA methylation, cells were treated daily with 1 μM 5-AzaC for 72 or 120 h. For the 120 h treatment, medium was replaced after 72 h with fresh medium containing 1 μM 5-AzaC.

Chromatin Immunoprecipitation Assay. Immunoprecipitation of chromatin was performed as described (*29*) with minor modifications. Erythroid maturation of MEL cells was induced by treatment of 0.5×10^5 cells/mL with 1.5% DMSO (Sigma) for 4 days. Uninduced MEL cells were plated at the same density and grown for 4 days without DMSO. Cross-linking was done by incubating cells (1×10^7 per condition) with a final concentration of 0.4% formaldehyde for 10 min at room temperature with agitation. Reactions were terminated by the addition of 125 mM glycine for 5 min at room temperature. Cells were collected by centrifugation at 240*g* for 6 min and washed in ice-cold PBS. Nuclei were isolated by incubation in cell lysis buffer (10 mM Tris-HCl, 10 mM NaCl, 0.2% Nonidet P-40, 10 mM sodium butyrate, 1 μg/mL leupeptin, and 50 μg/mL PMSF, pH 8.1) for 10 min on ice, followed by centrifugation for 2 min at 600*g*. Nuclei were lysed in nuclei lysis buffer (50 mM Tris-HCl, 10 mM EDTA, 1% SDS, 10 mM sodium butyrate, 1 μg/mL leupeptin, and 50 μg/mL PMSF, pH 8.1) for 10 min at 4 °C. The lysate was sonicated with eight pulses of 30 s each at 60% of maximum power with a Heat Wave Systems W185F sonicator (Ultrasonics, Farmingdale, NY) to reduce chromatin fragments to an average size of ~500 bp. After centrifugation at 16000*g* for 10 min, soluble chromatin was diluted with immunoprecipitation (IP) dilution buffer (20 mM Tris-HCl, 150 mM NaCl, 2 mM EDTA, 0.01% SDS, 1% Triton X-100, 10 mM sodium butyrate, 1 μg/mL leupeptin, and 50 μg/mL PMSF, pH 8.1) at a 1:4 ratio of nuclei lysis buffer to IP dilution buffer. Chromatin was then precleared by incubation with 50 μL of preimmune serum for 1 h, followed by 100 μL of protein A−Sepharose for at least 12 h. Aliquots of precleared samples (input) were saved. Remaining samples were incubated with 7 μL of the relevant antibody in a final volume of 0.9 mL for 3 h at 4

[1] Abbreviations: 5-AzaC, 5-azacytidine; ChIP, chromatin immunoprecipitation; DMSO, dimethyl sulfoxide; DNase I, deoxyribonuclease I; DTT, dithiothreitol; EDTA, ethylenediaminetetraacetic acid; EKLF, erythroid kruppel-like factor; H3-meK4, methylated lysine 4 of histone H3; H3-meK9, methylated lysine 9 of histone H3; HAT, histone acetyltransferase; HDAC, histone deacetylase; LCR, locus control region; MEL, mouse erythroleukemia; PBS, phosphate-buffered saline; PCR, polymerase chain reaction; PMSF, phenylmethanesulfonyl fluoride; SDS, sodium dodecyl sulfate; Tris, tris(hydroxymethyl)aminomethane; TSA, trichostatin A.

°C. Immune complexes were collected by incubation with 30 μL of protein A−Sepharose for 2 h at 4 °C. Sepharose beads were washed twice with 0.5 mL aliquots of IP wash buffer 1 (20 mM Tris-HCl, 50 mM NaCl, 2 mM EDTA, 0.1% SDS, and 1% Triton X-100, pH 8.1), once with IP wash buffer 2 (10 mM Tris-HCl, 0.25 M LiCl, 1 mM EDTA, 1% Nonidet P-40, and 1% deoxycholate, pH 8.1), and twice with TE buffer (10 mM Tris-HCl and 1 mM EDTA, pH 8.0). Immune complexes were eluted twice with 150 μL of IP elution buffer (0.1 M $NaHCO_3$ and 1% SDS). Cross-links were reversed by adding RNase A (3.3 μg/mL) and NaCl (0.3 M) and incubating for 4−5 h at 65 °C. Samples were digested with proteinase K (0.2 mg/mL) for at least 2 h at 45 °C. DNA was purified by extraction with phenol/chloroform (once and twice for immunoprecipitated and input samples, respectively) and once with chloroform, followed by ethanol precipitation. Purified DNA was resuspended in 30 μL (IP sample) or 66.7 μL (input) of 10 mM Tris-HCl (pH 8.0).

Aliquots of immunoprecipitated chromatin (1.5 μL) were analyzed by real-time PCR as described (*51*). Primers were designed by Primer Express 1.0 software (PE Applied Biosystems) to amplify 50−150 bp subregions within the corresponding standard PCR primers (*32*). Samples from at least two independent immunoprecipitations were analyzed in duplicate.

ChIP primer pairs were based on Hbb^d haplotype sequences (GenBank accession numbers Z13985, X14061, AF128269, and AF133300). Real-time PCR primers are as follows (5′−3′): HS2, AGTCAATTCTCTACTCCCCACCCT and ACTGCTGTGCTCAAGCCTGAT; IVR3, TGTGCTAGCCTCAAGCTCACA and TCCCAGCACTCAGAAGAAGGA; IVR5, GTATGCTCAATTCAAATGTACCTTATTTTAA and TTACCTCTTTATTTCACTTTTACACATAGCTAA; IVR16, TGGCCATTTTTACTATGTTAATTTTTGC and TAGACTTGTCATGGTTATGGATTGG; Ey, ATGACCTGGCTCCACCCAT and TCTTTGAAGCCATTGGTCAGC; *necdin*, GGTCCTGCTCTGATCCGAAG and GGGTCGCTCAGGTCCTTACTT; *cad*, TTCTAACTTGACCGGCTGGTTT and GGACCATAGGATGGTTCCACAG.

Restriction Endonuclease Accessibility and DNA Methylation Assays. DMSO-induced MEL cells were treated with and without 165 nM TSA for 4 h. Cells were collected by centrifugation at 240*g* for 6 min at 4 °C. Cells were washed with ice-cold PBS and resuspended in 1.5 volumes of lysis buffer (10 mM Tris-HCl, 10 mM NaCl, 3 mM $MgCl_2$, 0.2% Nonidet P-40, and 10 mM DTT, pH 7.5) and incubated for 10 min at 4 °C. Nuclei were collected by centrifugation at 600*g* for 2 min, resuspended in wash buffer (10 mM Tris-HCl, 10 mM NaCl, 3 mM $MgCl_2$, and 10 mM DTT, pH 7.5), and collected again by centrifugation. Nuclei were resuspended in 1× New England Biolabs restriction enzyme buffer 2 at 2×10^7 nuclei/0.2 mL. Restriction enzyme was added to aliquots, which were incubated for 45 min at 37 °C. Reactions were terminated by adding 10 mM Tris-HCl, 25 mM EDTA, and 1% SDS, pH 7.5. Proteinase K (0.4 mg/mL) was added, and samples were incubated overnight at 37 °C. DNA was purified by multiple phenol/chloroform extractions and one extraction with chloroform, followed by ethanol precipitation. Equal amounts of DNA (15 μg) were digested with secondary restriction enzymes. Samples were resolved on a 1.1% agarose gel, and Southern blotting was done with high specific activity, random-primed probes to identify parental bands and fragments.

For analysis of CpG dinucleotide methylation, genomic DNA (15 μg) was cleaved with *Msp*I or *Hpa*II in combination with restriction enzymes to generate an appropriate parental band. DNA was resolved on a 1.1% agarose gel. Parental bands and fragments were detected by Southern blotting with high specific activity, random-primed probes.

Antibodies. Anti-acetylated histone H3 (Upstate Biotechnology, 06-599), anti-acetylated histone H4 (Upstate Biotechnology, 06-899), and anti-dimethylated lysine 4, histone H3 (Upstate Biotechnology, 07-030) were used for ChIP assays. These antibodies react with multiple acetylated forms of H3 and H4, respectively. Rabbit anti-rat IgG (312-005-003) was obtained from Jackson Immunochemicals. Rabbit IgG and preimmune serum (PI) were controls.

Probes. Probes for restriction endonuclease accessibility and DNA methylation assays, corresponding to specific regions of the murine β-globin locus, were generated by PCR from the plasmid 129LC and pBELOBACAsp718 (gift from Dr. Steven Fiering, Dartmouth Medical School) templates. The probe coordinates are based on sequence data from the Globin Gene Server (*52*): HS2 (11433−11959); Ey (21213−21629); IVR3 (23623−24154).

RESULTS

Trichostatin A Preferentially Induces H4 Acetylation throughout the Central Subdomain of the Murine β-Globin Locus. Establishment and maintenance of H3 hypoacetylation and low-level H4 acetylation within the central subdomain of the murine β-globin locus might involve impaired HAT access or efficient attraction of HDACs. We showed that the HDAC inhibitor butyrate preferentially increased H4 acetylation at the *Ey*, but not the *βmajor*, promoter, suggesting that establishment and maintenance of low-level H4 acetylation at the *Ey* promoter requires HDACs (*32*). We have used a quantitative, real-time PCR-based ChIP assay (*51*) to ask whether this HDAC requirement is unique to promoters or if establishment and maintenance of hypoacetylation throughout the subdomain (Figure 1A) requires HDACs. HDACs were inhibited by TSA rather than butyrate, since TSA specifically inhibits all known HDACs except Sir2p (*44*). MEL cells were treated with TSA or vehicle for 4 h to induce bulk histone hyperacetylation. The sonicated chromatin used for ChIP had an average size of less than ∼500 bp (Figure 1B). Signals were proportional to the amount of input DNA (Figure 1C). Treatment of DMSO-induced MEL cells with TSA strongly increased H4 acetylation at the intergenic site IVR3 (14.2-fold) (Figure 1D). Dissociation analysis confirmed that SYBR Green fluorescence reflected the generation of a homogeneous PCR product (Figure 1E).

Histone acetylation was measured at distinct functional sites within the β-globin locus, including HS2, embryonic/fetal erythroid cell-specific *Ey* and brain-specific *necdin* promoters, and intergenic regions IVR3, IVR5, and IVR16 (Figure 2). IVR3 and IVR5 are representative intergenic sites within the central subdomain, while IVR16 is a representative intergenic site at the 3′-end of the locus (*32*). DMSO-induced MEL cells had high H3 and H4 acetylation at HS2 and low acetylation at the *Ey* promoter, IVR3, IVR5, and IVR16 and

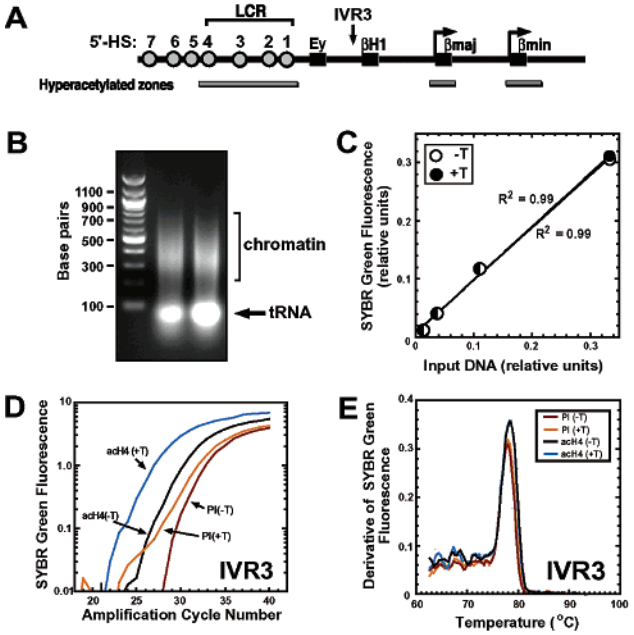

FIGURE 1: Quantitative real-time PCR assay to measure histone acetylation at the endogenous murine β-globin locus. (A) Organization of the murine β-globin locus containing the embryonic (*Ey* and *βH1*) and fetal/adult (*βmajor* and *βminor*) β-globin genes. β-Globin genes are shown as boxes and DNase I hypersensitive sites (HS) as spheres. The intergenic site analyzed is denoted IVR3. (B) Agarose gel analysis of sonicated, deproteinized chromatin used in the ChIP assay. Chromatin fragments smaller than 1 kb, averaging ~500 bp, were visualized by ethidium bromide staining. (C) Standard curves of SYBR Green fluorescence signals obtained from dilutions of input DNA from untreated (−T) and TSA-treated (+T), induced MEL cells. (D) Representative amplification plot of H4 acetylation (acH4) at IVR3 in untreated and TSA-treated MEL cells; PI, preimmune. (E) Dissociation plot obtained from amplicon shown in panel D. The single peak indicates the generation of a single amplicon.

at the brain-specific *necdin* promoter (Figure 2). TSA treatment strongly increased H4 acetylation at IVR3 (8.7-fold), IVR5 (15.3-fold), and the *Ey* promoter (7.9-fold). TSA induced H4 acetylation to a lesser degree at IVR16 (4.4-fold), downstream of *βminor*, and only slightly affected acetylation at HS2 (1.9-fold) and the *necdin* promoter (1.4-fold). Thus, the HDAC requirement to maintain low-level H4 acetylation is not specific for the *Ey* promoter, but rather low-level H4 acetylation is also maintained at intergenic sites within the central subdomain by HDACs.

H3 acetylation at all sites tested, with the exception of IVR5 (6.9-fold increase), was nonresponsive or weakly responsive to TSA (Figure 2). Thus, either HATs that establish H3 acetylation cannot access sites within the central subdomain or a TSA-resistant HDAC maintains H3 hypoacetylation. IVR5 differs from the other intergenic sites in that it resides near (1061 bp upstream) the H3 and H4 hyperacetylated *βmajor* promoter. HATs that establish H3 hyperacetylation at *βmajor* might exert a broader action on the adjacent region upon HDAC inhibition, explaining the unique response at IVR3.

Requirements for Establishment and Maintenance of Low-Level H4 Acetylation at the Central Subdomain of the Murine β-Globin Locus. The current paradigm for how HDACs access specific chromosomal sites involves targeted HDAC recruitment via protein−protein interactions with DNA-bound factors (*53*, *54*). Sequence analysis revealed that the intergenic sites tested are poorly conserved between mouse and man and lack known *cis* elements, which could serve as binding sites for repressors that directly recruit HDACs. Thus, HDACs recruited at distant sites might gain access to the intergenic sites, or HDACs might access the intergenic sites directly via a previously undescribed mechanism.

Similar to targeted HDAC recruitment, HATs localize to specific chromosomal sites by interaction with sequence-specific DNA binding proteins (*38*). Since TSA induces H4 hyperacetylation at multiple sites within the central subdomain, HATs can access the subdomain efficiently when HDAC activity is blocked. We reasoned that HATs recruited to the LCR and to other regulatory sites within the locus would gain access to the subdomain. Thus, *trans*-acting factors required for HAT recruitment would be critical for establishment of H4 hyperacetylation within the subdomain. P45/NF-E2 (*55*), GATA-1 (*56*), and EKLF (*57*) represent three hematopoietic-specific factors known to regulate the β-globin genes (*58*). P45/NF-E2 and GATA-1 bind multiple HSs of the LCR *in vivo* (*51*, *59*−*61*), and EKLF functions

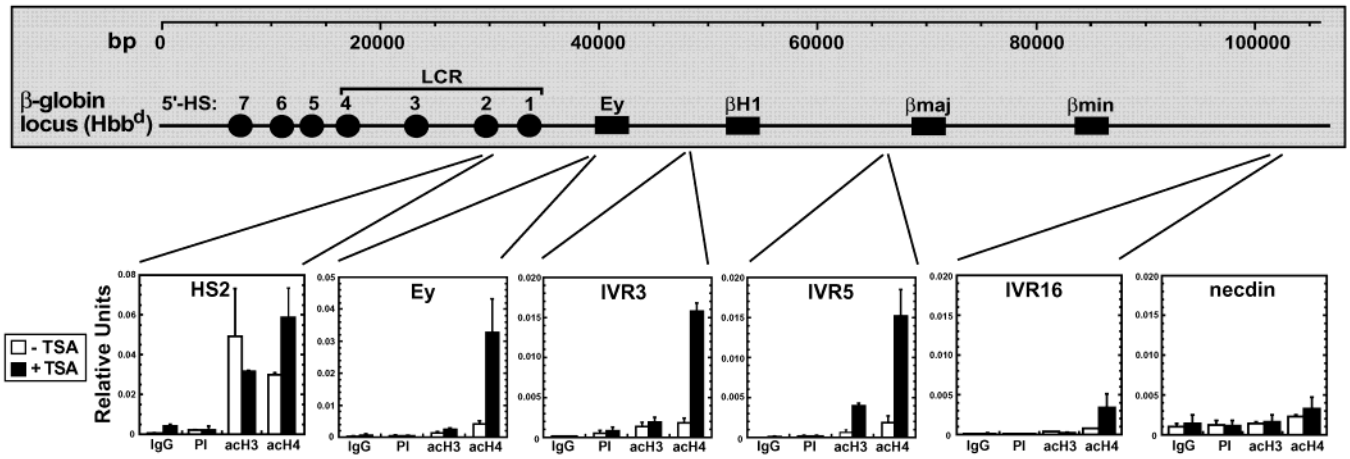

FIGURE 2: Trichostatin A preferentially induces H4 acetylation within the central subdomain of the murine β-globin locus. β-globin genes are shown as boxes and HS as spheres. Cross-linked chromatin was isolated from untreated and TSA-treated, DMSO-induced MEL cells. The relative levels of H3 and H4 acetylation obtained from quantitative ChIP analysis were plotted as a function of the position within the locus. Each point represents the mean from at least three independent experiments.

through HS3 (*62*). These factors interact with the HAT CBP/p300 (*63*−*66*) and therefore are candidates for factors that induce HAT recruitment to the locus.

To determine if p45/NF-E2, GATA-1, and EKLF are required for TSA-induced H4 hyperacetylation within the central subdomain, we used erythroid cell lines lacking these factors. CB3 cells were derived from the fetal liver of Friend erythroleukemia virus-infected mice (*47*), similar to MEL cells. However, in CB3 cells, Friend virus is integrated in one allele of *p45/NF-E2*, and the second allele is lost. P45/NF-E2 expression in CB3 cells reactivates the silenced fetal/adult β-globin genes (*47*, *67*). G1E cells were derived from GATA-1-null murine embryonic stem cells (*50*). These cells recapitulate the phenotype of a normal proerythroblast. GATA-1 expression in G1E cells strongly induces fetal/adult β-globin expression and terminal erythroid differentiation. EKLF-null B1 cells were also derived from murine ES cells. EKLF expression in B1 cells strongly induces fetal/adult β-globin expression and induces terminal erythroid differentiation (*49*).

If p45/NF-E2, GATA-1, or EKLF is required to recruit HATs that access the central subdomain upon TSA treatment, preferential induction of H4 hyperacetylation should be impaired in the null cells. Quantitative ChIP analysis revealed that TSA treatment induced H4 hyperacetylation at IVR3 in the null cells (CB3, 3.5-fold increase; G1E, 9.8-fold; B1, 7.9-fold) (Figure 3). Similar to the results of Figure 2, TSA had little or no effect on H3 and H4 acetylation at HS2. One exception to this was apparent in G1E cells, in which TSA increased H4 acetylation 2.6-fold at HS2. Thus, upon HDAC inhibition, HATs that establish H4 hyperacetylation retain the ability to access the central subdomain in cells lacking p45/NF-E2, GATA-1, or EKLF.

The experiments of Figure 2 used MEL cells treated with DMSO to induce erythroid maturation. The MEL cell line used in our laboratory expresses GATA-1 equivalently in uninduced and DMSO-induced cells, while p45/NF-E2 expression increases upon induction (*68*). Since β-globin expression is considerably lower in uninduced versus induced MEL cells, erythroid cell differentiation-dependent signals are required to maximally activate the fetal/adult β-globin genes. In principle, such signals might allow HAT access to the central subdomain upon HDAC inhibition. We analyzed the histone acetylation state of HS2 and IVR3 in untreated and TSA-treated, uninduced MEL cells (Figure 3). In uninduced cells, TSA induced H4 hyperacetylation at IVR3 (3.5-fold) but had little effect on H4 hyperacetylation at HS2 (1.2-fold). This result indicates that HAT access to the central subdomain does not require differentiation-dependent signals. However, since the increase observed at IVR3 in DMSO-induced MEL cells was 8.7-fold, such signals might amplify the hyperacetylation response.

The results of Figure 3 raise the question of whether any erythroid cell-specific factors are required to establish H4 hyperacetylation at the central subdomain. To assess this, quantitative ChIP analysis was conducted to measure H3 and H4 acetylation at IVR3 and at the *cad* and *necdin* promoters in murine L1210 lymphocytic leukemia cells, which do not express β-globin genes. H3 and H4 acetylation was low at IVR3 and the *necdin* promoter, while acetylation was high at the *cad* promoter. TSA treatment only weakly (<2-fold)

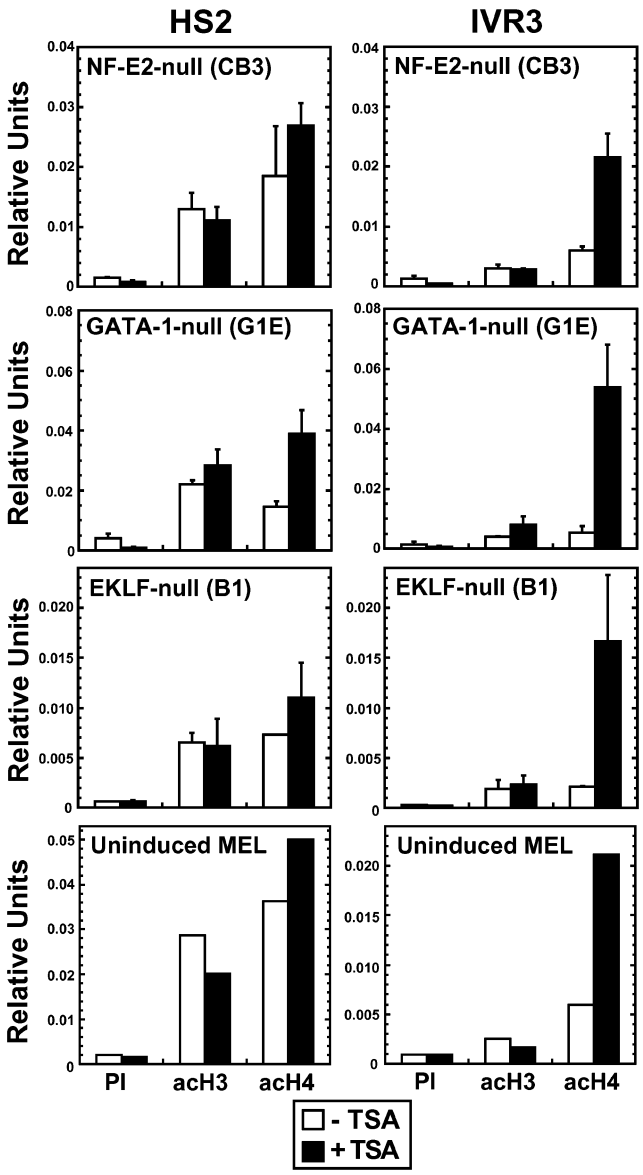

FIGURE 3: GATA-1, p45/NF-E2, and EKLF are not required for trichostatin A-dependent H4 hyperacetylation. Cross-linked chromatin was isolated from untreated and TSA-treated cell lines lacking the respective transcription factors (NF-E2-null, CB3 cells; GATA-1-null, G1E cells; EKLF-null, B1 cells) and also undifferentiated MEL cells. The relative levels of H3 and H4 acetylation (acH3 and acH4, respectively) at HS2 and IVR3 obtained from quantitative ChIP analysis were plotted. Each point represents the mean from three (NF-E2-, GATA-1-, and EKLF-null) and two (uninduced MEL) independent experiments. PI, preimmune.

increased H4 acetylation at these sites (Figure 4). As TSA strongly induced H4 hyperacetylation at IVR3 in erythroid cells (MEL, CB3, G1E, and EKLF-null, Figures 2 and 3) but not in nonerythroid L1210 cells, establishment and/or maintenance of H4 hyperacetylation within the central subdomain appears to require erythroid cell-specific factors.

Chromatin Architecture of the Central Subdomain of the Murine β-Globin Locus. The central subdomain in which the *Ey* and *βH1* genes reside is characterized by H3 hypoacetylation and low-level H4 acetylation. Low-level acetylation is a hallmark feature of "inactive" chromatin. However, additional parameters of the chromatin architecture of this region have not been investigated, and therefore, it is unclear whether the chromatin of the central subdomain

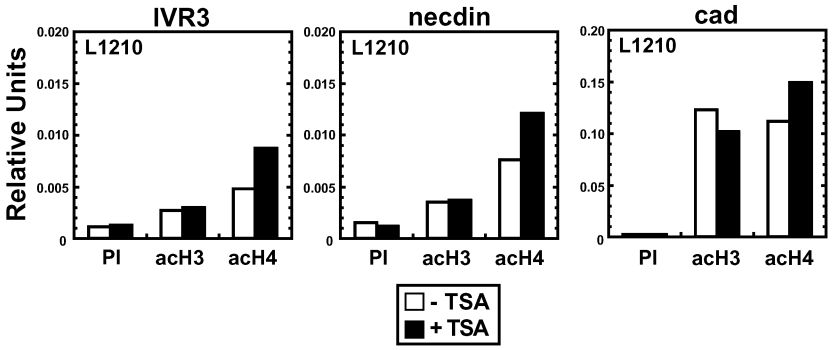

FIGURE 4: Trichostatin A does not induce H4 hyperacetylation at IVR3 in L1210 lymphocytic leukemia cells. Cross-linked chromatin was isolated from untreated and TSA-treated L1210 cells. The relative levels of H3 and H4 acetylation (acH3 and acH4, respectively) at IVR3 and the *necdin* and *cad* promoters obtained from quantitative ChIP analysis were plotted. Each point represents the mean from two independent experiments. PI, preimmune.

represents "inactive" chromatin within an active tissue-specific domain. It seems reasonable to assume that induction of H4 hyperacetylation would increase cis-element accessibility and might trigger additional chromatin structure changes. To investigate these possibilities, we measured chromatin accessibility with a restriction endonuclease accessibility assay (*69*). Nuclei were isolated from control and TSA-treated, DMSO-induced MEL cells and were incubated with *Hae*III. Cleavage at HS2 and the *Ey* promoter was measured by Southern blotting and Phosphorimager analysis. HS2 and the *Ey* promoter each contain two *Hae*III sites within *Eco*RI and *Xba*I−*Eco*RI parental fragments, respectively (Figure 5A). *Hae*III only weakly cleaved the *Ey* promoter in nuclei from DMSO-induced MEL cells (5% of templates cleaved), while *Hae*III cleaved ∼50% of the templates at HS2 (Figure 5B,C). TSA treatment did not increase cleavage at either site. As TSA strongly induces H4 acetylation at the *Ey* promoter (Figure 2), H4 hyperacetylation is insufficient to generate highly accessible chromatin at this site.

Since H4 hyperacetylation did not increase *Hae*III accessibility, additional structural features of the chromatin besides low-level H4 acetylation must be required to maintain the inaccessible state of the central subdomain. CpG dinucleotide methylation is an important feature of "inactive" chromatin (*70*) and has been implicated in the control of chicken β-globin gene switching (*71*−*73*). The chicken embryonic ρ-globin promoter and proximal transcribed region is completely unmethylated in expressing embryonic erythroid cells, while it is methylated in nonexpressing adult erythroid cells (*72*, *73*). It was hypothesized that methylation is not a critical determinant of ρ-globin silencing during erythropoiesis but rather functions at a step postsilencing to maintain repression.

CpG methylation can be readily measured by use of the restriction endonucleases *Hpa*II and *Msp*I. These endonucleases differentially cleave a common recognition site, CCGG. *Msp*I cleaves regardless of the methylation state of the site, whereas *Hpa*II cleaves only the unmethylated site. Southern blot analysis of genomic DNA isolated from control and TSA-treated, DMSO-induced MEL cells revealed nearly complete methylation of two *Hpa*II/*Msp*I sites within an *Eco*RI fragment downstream of *Ey* (Figure 6A). TSA has been shown to induce demethylation of a promoter within a transiently transfected cytomegalovirus-enhanced green fluorescent protein plasmid in HEK293 cells (*74*, *75*). However, TSA treatment did not induce demethylation at the *Hpa*II/*Msp*I sites within the central subdomain (Figure 6B). Thus, H4 hyperacetylation resulting from HDAC inhibition does

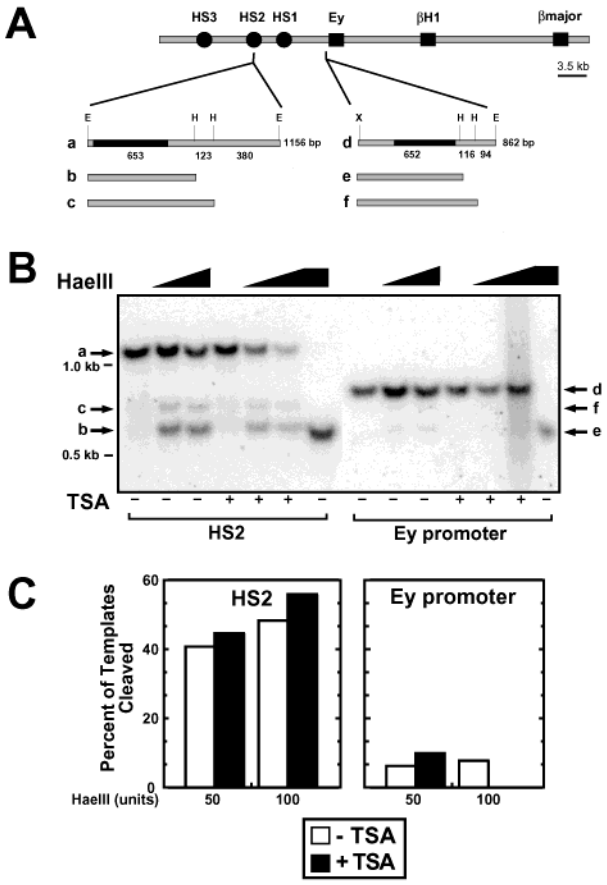

FIGURE 5: Chromatin at the *Ey* promoter is inaccessible to *Hae*III in isolated nuclei and H4 hyperacetylation does not increase accessibility. Nuclei isolated from untreated and TSA-treated, DMSO-induced MEL cells were incubated with the restriction endonuclease *Hae*III for 45 min at 37 °C. *Hae*III cleavage was measured by Southern blotting. (A) Map of the murine β-globin locus showing restriction sites near HS2 and *Ey*, which were used for the Southern blotting strategy. β-Globin genes are shown as boxes and HS as spheres. Probes are denoted by black bars. All possible fragments are depicted and labeled as a−f. E, *Eco*RI; H, *Hae*III; X, *Xba*I. (B) Representative Southern blot. Fragments are identified by arrows, corresponding to the fragments of panel A. Lanes 7 and 14 show purified genomic DNA digested to completion with *Hae*III/*Eco*RI and *Hae*III/*Xba*I/*Eco*RI, respectively. (C) Quantitative analysis. Band intensities were quantitated by Phosphorimager analysis. The graphs depict mean values from two independent experiments.

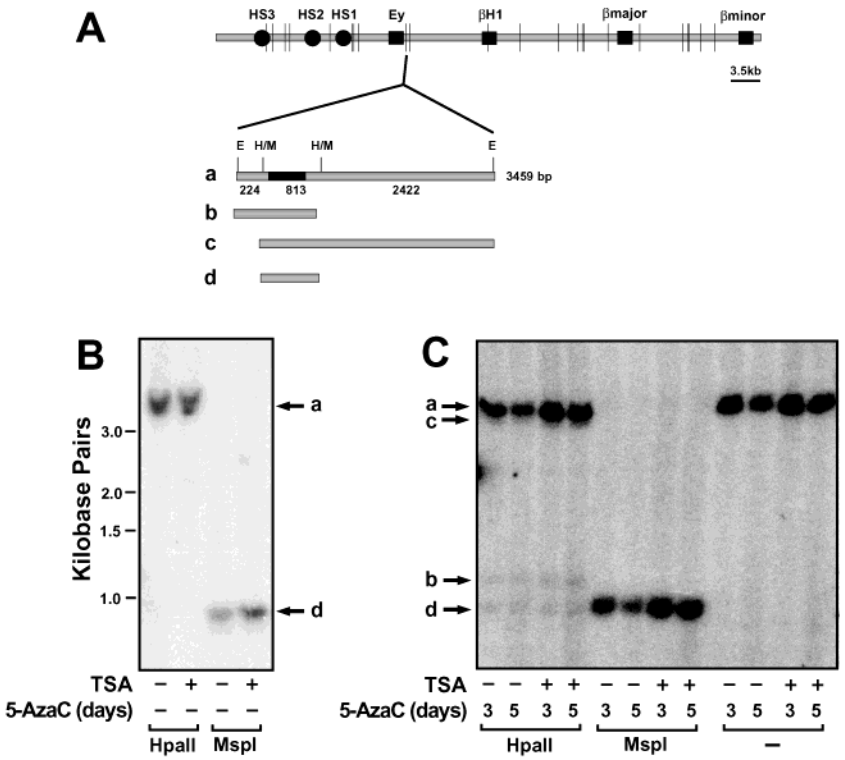

FIGURE 6: Trichostatin A and 5-AzaC do not synergistically induce demethylation of highly methylated chromatin near *Ey*. Genomic DNA was isolated from untreated and TSA-treated, DMSO-induced MEL cells (B) and untreated, TSA-treated, and 5-AzaC-treated, uninduced MEL cells (C). Purified DNA was digested with *Hpa*II (methylation-sensitive) and *Msp*I (methylation-insensitive) restriction endonucleases, in combination with *Eco*RI, and analyzed by Southern blotting. (A) Map of the murine β-globin locus showing restriction sites 3′ of *Ey*, which were used for the Southern blotting strategy. β-Globin genes are shown as boxes and HS as spheres. The probe is denoted by a black bar. All possible fragments are depicted and labeled a−d. Vertical lines depict *Hpa*II/*Msp*I sites. E, *Eco*RI; H/M, *Hpa*II/*Msp*I. (B, C) Representative Southern blots. Fragments are identified by arrows, corresponding to the fragments of panel A.

not increase *Hae*III accessibility, nor does it reverse DNA methylation within the central subdomain.

TSA synergizes with 5-AzaC to reactivate silenced genes in cancer cells (*76*−*79*). However, this synergism has not been observed in all systems (*80*). Since the results of Figure 6B show that CpG sites within the central subdomain are highly methylated and that TSA does not induce demethylation, we asked whether TSA and 5-AzaC synergistically induce demethylation. Treatment of MEL cells with 5-AzaC induced low-level demethylation (19%) (Figure 6C), which was not enhanced by varying the 5-AzaC concentration (1−10 μM) and incubation time (1−5 days) (data not shown). Induction of H4 hyperacetylation by TSA treatment did not increase the degree of demethylation, indicating that TSA and 5-AzaC do not synergistically induce demethylation of *Hpa*II/*Msp*I sites within the central subdomain.

Multiple studies have provided evidence for links between establishment of distinct histone modifications (*26*). However, no reports have described the influence of preferential H4 hyperacetylation, without concomitant H3 hyperacetylation, on other histone modifications. Besides acetylation, methylated lysine 4 of histone H3 (H3-meK4) is enriched in "active" chromatin (*81*, *82*). We showed that H3-meK4 is strongly enriched at HS2 and at the fetal/adult β-globin genes but is undetectable at IVR3 (*83*). We asked whether induction of H4 hyperacetylation was linked to a concomitant increase in H3-meK4. While TSA treatment slightly increased H3-meK4 at HS2, TSA did not induce H3-meK4 at IVR3 (Figure 7). This result provides evidence that restoration of one component of the "active" chromatin structure

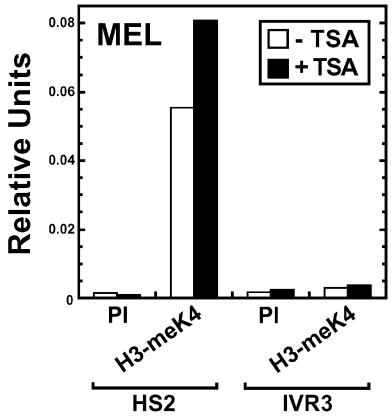

FIGURE 7: H4 hyperacetylation and H3-meK4 are not established concomitantly. Quantitative ChIP analysis of H3-meK4 at HS2 and IVR3 of untreated and TSA-treated, DMSO-induced MEL cells. Each point represents the mean from two independent experiments. PI, preimmune; H3-meK4, methylated lysine 4 of histone H3.

of the locus is not linked to an increase in another component, H3-meK4.

DISCUSSION

HDAC-Dependent Surveillance Mechanism for Establishment of Low-Level Histone Acetylation over a Long Distance on a Chromosome. Intriguingly, despite the fact that TSA induces bulk H3 and H4 acetylation, TSA preferentially increases H4 acetylation throughout a ∼30 kb central subdomain within the erythroid-specific β-globin domain. We propose a surveillance mechanism in which HDACs

continually scan this region, thereby maintaining low-level H4 acetylation. Attraction of HATs and HDACs to the central subdomain does not require the hematopoietic-specific transcription factors p45/NF-E2, GATA-1, and EKLF (Figure 3), which function through *cis* elements of the β-globin locus. Erythroid cell-specific factors are required, however, as determined by TSA-dependent hyperacetylation in multiple erythroid cell lines and the failure of TSA to induce hyperacetylation in L1210 cells (Figure 4). These factors might induce targeted recruitment of HATs and HDACs to the subdomain. Alternatively, HATs and HDACs might access the central subdomain via relocalization from adjacent sites or changes in the subnuclear localization of the β-globin locus (*84*).

The degree of H4 hyperacetylation achieved upon TSA treatment at IVR16 (Figure 2) was considerably lower than at IVR3 and IVR5. IVR16 resides more than 10 kb downstream of the hyperacetylated zone at the *βminor* gene, while IVR3 and IVR5 reside in the central subdomain, flanked by the hyperacetylated zones at the LCR and at the *βmajor* gene. The greater hyperacetylation response at IVR3 and IVR5 would be consistent with a model in which HATs emanate from hyperacetylated zones, and IVR16 is simply too far from hyperacetylated zones for HATs to efficiently access.

If broad hypoacetylation does not result from targeted recruitment via HDAC-repressor interactions, how might HDACs be attracted to the central subdomain? Since the DNA at two sites examined within the subdomain was highly methylated, 5-methylcytosine might be critical for recruiting HDACs. HDACs are known to physically interact with methyl CpG binding proteins (*85*−*89*). Moreover, TSA and 5-AzaC synergistically reactivate certain silenced genes (*76*, *77*, *79*). Thus, HDACs can, in principle, be recruited to a broad chromosomal region by use of methylated DNA binding proteins as a bridge. Nevertheless, targeting of HDACs to methylated DNA has not been shown to underlie the establishment of broad hypoacetylation. The results of Figure 6 showing that TSA-induced H4 hyperacetylation does not stimulate DNA demethylation is consistent with a mechanism in which methylation can occur independently of H4 acetylation/deacetylation. TSA also did not reactivate a methylated chicken *ρ-globin* construct transfected into erythroid cells (*73*).

A critical prediction of a surveillance mechanism in which HDACs continually access methylated DNA is that perturbation of methylation would preclude HDAC recruitment. However, 5-AzaC was inefficient in inducing demethylation of sites within the central subdomain, and TSA did not potentiate 5-AzaC-induced demethylation (Figure 6C). Thus, the methylated state exhibits high stability, which might reflect the absence of factors in adult erythroid cells required for establishment and maintenance of the demethylated state.

Dissection of Multiple Steps in Assembly of the Inaccessible Chromatin Structure of the Central Subdomain. Although we previously described the broad low-level acetylation of the central subdomain of the murine β-globin locus (*32*), other parameters of chromatin structure at this subdomain had not been measured. The restriction endonuclease accessibility result (Figure 5) provided strong evidence that sites within this subdomain are largely inaccessible to endonucleases (Figure 5). TSA-induced H4 hyperacetylation did not increase restriction endonuclease accessibility at the *Ey* promoter (Figure 5), nor did it increase H3-meK4 at IVR3 (Figure 7). Moreover, we have shown that GATA-1 does not associate with consensus sites within the central subdomain (*51*), and TSA does not induce GATA-1 recruitment to these sites (data not shown). As hyperacetylation is believed to enhance chromatin accessibility, these results were unexpected. However, we are unaware of reports examining the impact of preferential H4 acetylation, without concomitant H3 acetylation, on chromatin accessibility.

The results described herein suggest that establishment of the inaccessible structure, in which the silent *Ey* and *βH1* genes reside, requires at least three components: TSA-sensitive, HDAC-dependent H4 deacetylation; TSA-insensitive, HDAC-dependent H3 deacetylation or impaired access of HATs that establish H3 acetylation; and induction of DNA methylation. The development of cell-free assays, potentially with isolated nuclei, will complement *in vivo* approaches to analyzing mechanisms underlying the establishment and maintenance of the central subdomain. Such mechanistic studies should allow one to test the HDAC surveillance model and to determine if this model has broad relevance for how histone modification patterns are established and maintained over a long distance on a chromosome.

ACKNOWLEDGMENT

We thank Yaakov Ben-David and Mitchell Weiss for CB3 and G1E cells, respectively. We thank Steven Fiering for the 129LC plasmid and pBELOBACAsp718. We also thank Kirby Johnson and Carol Kiekhaefer for a critical review of the manuscript.

REFERENCES

1. Felsenfeld, G. (1992) *Nature 355*, 219−224.
2. van Holde, K. (1989) *Chromatin*, Springer-Verlag, New York.
3. Wolffe, A. (1995) *Chromatin*, Academic Press, New York.
4. Archer, T. K., Cordingley, M. G., Wolford, R. G., and Hager, G. L. (1991) *Mol. Cell. Biol. 11*, 688−698.
5. Pina, B., Bruggemeier, U., and Beato, M. (1990) *Cell 60*, 719−731.
6. Hager, G. L., Archer, T. K., Fragoso, G., Bresnick, E. H., Tsukagoshi, Y., John, S., and Smith, C. L. (1993) *Cold Spring Harbor Symp. Quant. Biol. 58*, 63−71.
7. Clark, D. J., and Kimura, T. (1990) *J. Mol. Biol. 211*, 883−896.
8. Yao, J., Lowary, P. T., and Widom, J. (1991) *Biochemistry 30*, 8408−8414.
9. Ericsson, C., Grossbach, U., Bjorkroth, B., and Daneholt, B. (1990) *Cell 60*, 73−83.
10. Owen-Hughes, T., and Workman, J. L. (1994) *Crit. Rev. Eukaryot. Gene Expression 4*, 403−441.
11. Weisbrod, S. (1982) *Nature 297*, 289−295.
12. Weintraub, H., and Groudine, M. (1976) *Science 193*, 848−856.
13. Stalder, J., Larsen, A., Engel, J. D., Dolan, M., Groudine, M., and Weintraub, H. (1980) *Cell 20*, 451−460.
14. Hebbes, T. R., Clayton, A. L., Thorne, A. W., and Crane-Robinson, C. (1994) *EMBO J. 13*, 1823−1830.
15. Lee, D. Y., Hayes, J. J., Pruss, D., and Wolffe, A. P. (1993) *Cell 72*, 73−84.
16. Vettese-Dadey, M., Grant, P. A., Hebbes, T. R., Crane-Robinson, C., Allis, C. D., and Workman, J. L. (1996) *EMBO J. 15*, 2508−2518.
17. Imai, B. S., Yau, P., Baldwin, J. P., Ibel, K., May, R. P., and Bradbury, E. M. (1986) *J. Biol. Chem. 261*, 8784−92.
18. Ausio, J., and van Holde, K. E. (1986) *Biochemistry 25*, 1421−8.
19. Bresnick, E. H., John, S., and Hager, G. L. (1991) *Biochemistry 30*, 3490−7.
20. Mutskov, V., Gerber, D., Angelov, D., Ausio, J., Workman, J., and Dimitrov, S. (1998) *Mol. Cell. Biol. 18*, 6293−6304.

21. Ridsdale, J. A., Hendzel, M. J., Delcuve, G. P., and Davie, J. R. (1990) *J. Biol. Chem. 265*, 5150−5156.
22. Tse, C., Sera, T., Wolffe, A. P., and Hansen, J. C. (1998) *Mol. Cell. Biol. 18*, 4629−4638.
23. Brown, C. E., Lechner, T., Howe, L., and Workman, J. L. (2000) *Trends Biochem Sci. 25*, 15−19.
24. Roth, S. Y., Denu, J. M., and Allis, C. D. (2001) *Annu. Rev. Biochem. 70*, 81−120.
25. Urnov, F. D., and Wolffe, A. P. (2001) *Oncogene 20*, 2991−3006.
26. Jenuwein, T., and Allis, C. D. (2001) *Science 293*, 1074−1080.
27. Forsberg, E. C., and Bresnick, E. H. (2001) *Bioessays 23*, 820−830.
28. Eberharter, A., and Becker, P. B. (2002) *EMBO Rep. 3*, 224−229.
29. Johnson, K. D., and Bresnick, E. H. (2002) *Methods 26*, 27−36.
30. Bulger, M., Sawado, T., Schubeler, D., and Groudine, M. (2002) *Curr. Opin. Genet. Dev. 12*, 170−177.
31. Litt, M. D., Simpson, M., Recillas-Targa, F., Prioleau, M. N., and Felsenfeld, G. (2001) *EMBO J. 20*, 2224−2235.
32. Forsberg, E. C., Downs, K. M., Christensen, H. M., Im, H., Nuzzi, P. A., and Bresnick, E. H. (2000) *Proc. Natl. Acad. Sci. U.S.A. 97*, 14494−14499.
33. Schubeler, D., Francastel, C., Cimbora, D. M., Reik, A., Martin, D. I., and Groudine, M. (2000) *Genes Dev. 14*, 940−950.
34. Forrester, W. C., Takegawa, S., Papayannopoulou, T., Stamatoyannopoulos, G., and Groudine, M. (1987) *Nucleic Acids Res. 15*, 10159−10177.
35. Grosveld, F., van Assendelft, G. B., Greaves, D. R., and Kollias, G. (1987) *Cell 51*, 975−985.
36. Smith, R. D., Yu, J., and Seale, R. L. (1984) *Biochemistry 23*, 785−790.
37. Gribnau, J., Diderich, K., Pruzina, S., Calzolari, R., and Fraser, P. (2000) *Mol. Cell 5*, 377−386.
38. Brownell, J. E., Zhou, J., Ranalli, T., Kobayashi, R., Edmondson, D. G., Roth, S. Y., and Allis, C. D. (1996) *Cell 84*, 843−851.
39. Laherty, C. D., Yang, W. M., Sun, J. M., Davie, J. R., Seto, E., and Eisenman, R. N. (1997) *Cell 89*, 349−356.
40. Kadosh, D., and Struhl, K. (1998) *Mol. Cell. Biol. 18*, 5121−5127.
41. Heinzel, T., Lavinsky, R. M., Mullen, T. M., Soderstrom, M., Laherty, C. D., Torchia, J., Yang, W. M., Brard, G., Ngo, S. D., Davie, J. R., Seto, E., Eisenman, R. N., Rose, D. W., Glass, C. K., and Rosenfeld, M. G. (1997) *Nature 387*, 43−48.
42. Vignali, M., Steger, D. J., Neely, K. E., and Workman, J. L. (2000) *EMBO J. 19*, 2629−2640.
43. Imai, S. C., Armstrong, C. M., Kaeberlein, M., and Guarente, L. (2000) *Nature 403*, 795−800.
44. Furumai, R., Komatsu, Y., Nishino, N., Khochbin, S., Yoshida, M., and Horinouchi, S. (2001) *Proc. Natl. Acad. Sci. U.S.A. 98*, 87−92.
45. Guardiola, A. R., and Yao, T. P. (2002) *J. Biol. Chem. 277*, 3350−3356.
46. Marks, P. A., Sheffrey, M., and Rifkind, R. A. (1985) *Prog. Clin. Biol. Res. 191*, 185−203.
47. Lu, S. J., Rowan, S., Bani, M. R., and Ben-David, Y. (1994) *Proc. Natl. Acad. Sci. U.S.A. 91*, 8398−8402.
48. Goldin, A. (1969) *Cancer Res. 29*, 2285−2291.
49. Coghill, E., Eccleston, S., Fox, V., Cerruti, L., Brown, C., Cunningham, J., Jane, S., and Perkins, A. (2001) *Blood 97*, 1861−8.
50. Weiss, M. J., Yu, C., and Orkin, S. H. (1997) *Mol. Cell. Biol. 17*, 1642−1651.
51. Johnson, K. D., Grass, J. D., Boyer, M. E., Kiekhaefer, C. M., Blobel, G. A., Weiss, M. J., and Bresnick, E. H. (2002) *Proc. Natl. Acad. Sci. U.S.A. 99*, 11760−11765.
52. Riemer, C., ElSherbini, A., Stojanovic, N., Schwartz, S., Kwitkin, P. B., Miller, W., and Hardison, R. (1998) *Genomics 53*, 325−337.
53. Ayer, D. E. (1999) *Trends Cell. Biol. 9*, 193−198.
54. Grozinger, C. M., and Schreiber, S. L. (2002) *Chem. Biol. 9*, 3−16.
55. Andrews, N. C., Erdjument-Bromage, H., Davidson, M. B., Tempst, P., and Orkin, S. H. (1993) *Nature 362*, 722−728.
56. Tsai, S. F., Martin, D. I., Zon, L. I., D'Andrea, A. D., Wong, G. G., and Orkin, S. H. (1989) *Nature 339*, 446−451.
57. Miller, I. J., and Bieker, J. J. (1993) *Mol. Cell. Biol. 13*, 2776−2786.
58. Cantor, A. B., and Orkin, S. H. (2002) *Oncogene 21*, 3368−3376.
59. Forsberg, E. C., Downs, K. M., and Bresnick, E. H. (2000) *Blood 96*, 334−339.
60. Daftari, P., Gavva, N. R., and Shen, C. K. (1999) *Oncogene 18*, 5482−5486.
61. Duan, Z., Stamatoyannopoulos, G., and Li, Q. (2001) *Mol. Cell. Biol. 21*, 3083−3095.
62. Tewari, R., Gillemans, N., Wijgerde, M., Nuez, B., von Lindern, M., Grosveld, F., and Philipsen, S. (1998) *EMBO J. 17*, 2334−2341.
63. Cheng, X., Reginato, M. J., Andrew, N. C., and Lazar, M. A. (1997) *Mol. Cell. Biol. 17*, 1407−1416.
64. Forsberg, E. C., Johnson, K., Zaboikina, T. N., Mosser, E. A., and Bresnick, E. H. (1999) *J. Biol. Chem. 274*, 26850−26859.
65. Zhang, W., and Bieker, J. J. (1998) *Proc. Natl. Acad. Sci. U.S.A. 95*, 9855−9860.
66. Blobel, G. A., Nakajima, T., Eckner, R., Montminy, M., and Orkin, S. H. (1998) *Proc. Natl. Acad. Sci. U.S.A. 95*, 2061−2066.
67. Kotkow, K. J., and Orkin, S. H. (1995) *Mol. Cell. Biol. 15*, 4640−4647.
68. Johnson, K. D., Christensen, H. M., Zhao, B., and Bresnick, E. H. (2001) *Mol. Cell 8*, 465−471.
69. Bresnick, E. H., and Felsenfeld, G. (1994) *Proc. Natl. Acad. Sci. U.S.A. 91*, 1314−1317.
70. Ng, H. H., and Bird, A. (1999) *Curr. Opin. Genet. Dev. 9*, 158−163.
71. Groudine, M., and Weintraub, H. (1981) *Cell 24*, 393−401.
72. Singal, R., Ferris, R., Little, J. A., Wang, S. Z., and Ginder, G. D. (1997) *Proc. Natl. Acad. Sci. U.S.A. 94*, 13724−13729.
73. Singal, R., Wang, S. Z., Sargent, T., Zhu, S. Z., and Ginder, G. D. (2002) *J. Biol. Chem. 277*, 1897−1905.
74. Cervoni, N., and Szyf, M. (2001) *J. Biol. Chem. 276*, 40778−40787.
75. Cervoni, N., Detich, N., Seo, S. B., Chakravarti, D., and Szyf, M. (2002) *J. Biol. Chem. 277*, 25026−25031.
76. Cameron, E. E., Bachman, K. E., Myohanen, S., Herman, J. G., and Baylin, S. B. (1999) *Nat. Genet. 21*, 103−107.
77. El-Osta, A., Kantharidis, P., Zalcberg, J. R., and Wolffe, A. P. (2002) *Mol. Cell. Biol. 22*, 1844−1857.
78. Yang, X., Phillips, D. L., Ferguson, A. T., Nelson, W. G., Herman, J. G., and Davidson, N. E. (2001) *Cancer Res. 61*, 7025−7029.
79. Lorincz, M. C., Schubeler, D., Goeke, S. C., Walters, M., Groudine, M., and Martin, D. I. (2000) *Mol. Cell. Biol. 20*, 842−850.
80. McInerney, J. M., Nawrocki, J. R., and Lowrey, C. H. (2000) *Gene Ther. 7*, 653−63.
81. Litt, M. D., Simpson, M., Gaszner, M., Allis, C. D., and Felsenfeld, G. (2001) *Science 293*, 2453−2455.
82. Boggs, B. A., Cheung, P., Heard, E., Spector, D. L., Chinault, A. C., and Allis, C. D. (2002) *Nat. Genet. 30*, 73−76.
83. Kiekhaefer, C. M., Grass, J. A., Johnson, K. D., Boyer, M. E., and Bresnick, E. H. (2002) *Proc. Natl. Acad. Sci. U.S.A. 99*, 14309−14314.
84. Francastel, C., Schubeler, D., Martin, D. I., and Groudine, M. (2000) *Nat. Rev. Mol. Cell. Biol. 1*, 137−143.
85. Nan, X., Ng, H. H., Johnson, C. A., Laherty, C. D., Turner, B. M., Eisenman, R. N., and Bird, A. (1998) *Nature 393*, 386−389.
86. Ng., H. H., Zhang, Y., Hendrich, B., Johnson, C. A., Turner, B. M., Erdjument-Bromage, H., Tempst, P., Reinberg, D., and Bird, A. (1999) *Nat. Genet. 23*, 58−61.
87. Wade, P. A., Gegonne, A., Jones, P. L., Ballestar, E., Aubry, F., and Wolffe, A. P. (1999) *Nat Genet. 23*, 62−66.
88. Zhang, Y., Ng, H. H., Erdjument-Bromage, H., Tempst, P., Bird, A., and Reinberg, D. (1999) *Genes Dev. 13*, 1924−1935.
89. Robertson, K. D., Ait-Si-Ali, S., Yokochi, T., Wade, P. A., Jones, P. L., and Wolffe, A. P. (2000) *Nat. Genet. 25*, 338−342.

BI026786Q